

Removal of methylene blue from aqueous solution by mesoporous silicalite-1 synthesized using carboxymethyl cellulose as template

Sabarish Radoor (✉ sabarishchem@gmail.com)

King Mongkut's University of Technology North Bangkok <https://orcid.org/0000-0002-0420-0240>

Jasila Karayil

Government Women's Polytechnic College

Aswathy Jayakumar

King Mongkut's University of Technology North Bangkok

Jyothi Mannekote Shivanna

Dayananda Sagar College of Engineering

Jyotishkumar Parameswaranpillai

King Mongkut's University of Technology North Bangkok

Suchart Siengchin

King Mongkut's University of Technology North Bangkok

Research Article

Keywords: Mesoporous, Silicalite-1, Methylene blue, Adsorption, Kinetics

Posted Date: May 4th, 2021

DOI: <https://doi.org/10.21203/rs.3.rs-350391/v2>

License: © ⓘ This work is licensed under a Creative Commons Attribution 4.0 International License.

[Read Full License](#)

1 **Removal of methylene blue from aqueous solution by mesoporous**
2 **silicalite-1 synthesized using carboxymethyl cellulose as template**

3 Sabarish Radoor^{1*}, Jasila Karayil², Aswathy Jayakumar¹, Jyothi Mannekote Shivanna³
4 Jyotishkumar Parameswaranpillai¹, Suchart Siengchin^{1*}

5 *

6 1. Materials and Production Engineering, The Sirindhorn International Thai-German Graduate
7 School of Engineering (TGGS), King Mongkut's University of Technology North Bangkok,
8 Bangkok 10800, Thailand

9 2. Government Women's Polytechnic College, Calicut, Kerala, India

10 3. Department of Chemistry, Dayananda Sagar College of Engineering, Shavige Malleshwara
11 Hills, Kumaraswamy Layout, Bengaluru, 560078, India

12
13 *Corresponding authors:

14 Sabarish Radoor, Email: sabarishchem@gmail.com

15 Suchart Siengchin, Email: suchart.s.pe@tggs-bangkok.org

16
17 **Abstract**

18 In the present work, we have developed a mesoporous silicalite-1 using CMC as a template for
19 the removal of MB from aqueous solution. The synthesized silicalite-1 were characterised
20 using scanning electron microscopy (SEM), transmission electron microscopy (TEM), Fourier
21 transform infrared spectroscopy (FT-IR), X-ray diffraction (XRD), thermogravimetric analysis
22 (TGA), Energy-dispersive X-ray spectroscopy (EDX) and N₂ adsorption-desorption isotherm
23 (BET). XRD and FTIR analysis confirmed the formation of crystallinity and development of
24 MFI structure in the mesoporous silicalite-1. The adsorption of MB dye on mesoporous
25 silicalite-1 was conducted by batch adsorption method. The effect of various parameters such
26 as adsorbent dosage, initial dye concentration, contact time and temperature on the dye uptake
27 ability of silicalite-1 was investigated. The operating parameters for the maximum adsorption
28 are silicalite-1 dosage (0.1 wt%), contact time (240 min), initial dye concentration (10 ppm)
29 and temperature (30°C). The MB dye removal onto mesoporous silicalite-1 followed pseudo-
30 second-order kinetic and Freundlich isotherm. The silicalite-1 exhibits 86% removal efficiency

31 even after six adsorption-desorption cycle. Therefore, the developed mesoporous silicalite-1 is
32 an effective eco-friendly adsorbent for MB dye removal from aqueous environment.

33 **Keywords:** *Mesoporous; Silicalite-1; Methylene blue; Adsorption; Kinetics*

34 **Introduction**

35 In the last few decades, the quality of water is declining in an alarming rate. Dyes are one of
36 the major pollutants which deteriorate our water resources such as river, lake etc.[1-3]
37 Synthetic dyes constitute about 90% of the total dye used in various industries such as paints,
38 textiles, paper, printing, plastics and cosmetics [4-6]. Azo dye, anthraquinones dyes,
39 phthalocyanines and polymethines are the common examples of synthetic dyes which is
40 frequently employed for different application [7, 8]. Dye dissemination into water bodies is not
41 only aesthetically unpleasant but also causes some major issues such as low dissolved oxygen
42 (DO) level, high BOD level and obstruction for sunlight transmission through water[8-11].
43 Thus, it adversely affects the aquatic organism[11]. Dyes effluent also cause serious health risk
44 to humans such as hypersensitivity, allergy, asthma, kidney dysfunction, liver and brain
45 disorder [12-14]. Methylene blue (MB) are recalcitrant pollutant with cariogenic and
46 mutagenic nature. It is generally used for dyeing cotton, silk and wool. The structural formula
47 of MB is shown in figure 1. It causes several health issues such as eye burns, skin irritation,
48 vomiting and nausea to humans [15-17].

49 The excessive use of dye raises concern and hence its removal from aqueous effluent has
50 become a challenging topic for researchers and scientists. Researchers have designed several
51 novel materials for dye removal by adopting technologies such as adsorption, coagulation,
52 oxidation, filtration, ultrafiltration etc.[18-20]. Due to simplicity, low-cost and high efficiency,
53 adsorption is considered as one of the most effective method for dye removal [21, 22].
54 Activated carbon and nanoparticle are effective adsorbent for dye removal applications,
55 however due to high cost and low efficiency its large-scale usage is limited [23]. Recently,

56 various low-cost and eco-friendly adsorbent were reported for removing dyes from wastewater
57 including zeolites, kaolin, clay, montmorillonite, activated carbon, agricultural waste etc.[23-
58 28] Silicalite-1 belongs to family of zeolite and possesses aluminium free MFI type framework.
59 High surface area and porous nature enable it to use in different application such as adsorption,
60 catalyst and fine chemical industrial applications [29, 30].

61 Jing et al. [31] fabricated TiO₂ loaded silicalite-1 for degradation of rhodamine B. They
62 reported that adsorbent dosage plays a key role in dye removal efficiency as they observed a
63 significant increment in dye removal efficiency with adsorbent dosage. Cheng et al. [32]
64 reported that GO/silicalite-1 composite is as an effective adsorbent for rhodamine B. The
65 maximum adsorption capacity (56.55 mg/g) was observed at pH=3 within 30 min of contact
66 time. Recently, our team fabricated sodium alginate modified silicalite-1 for rhodamine B
67 removal. The modified silicalite-1 displayed high removal efficiency than conventional
68 silicalite-1 probably due to the high surface area and pore diameter. The reusability test was
69 also conducted to check the industrial advantage. The result proved that sodium alginate
70 modified silicalite-1 exhibits good regeneration capacity [33].

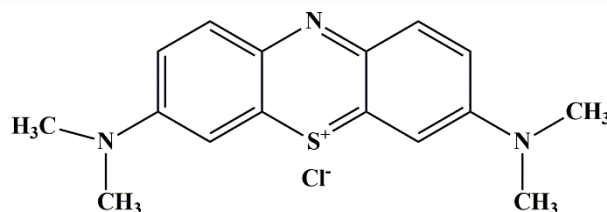
71 There is only limited research available for dye adsorption studies on silicalite-1 from
72 wastewater. So, in this work, we made an attempt to evaluate the dye (MB) adsorption capacity
73 of s carboxymethyl cellulose (CMC) modified silicalite-1. The effect of different parameters
74 such as initial dye concentration, contact time, temperature, dosage on the adsorption process
75 was also discussed in details. The adsorption kinetics and isotherm on adsorption process is
76 also presented.

77 **Materials and methods**

78 **Chemicals**

79 Tetrapropylammonium hydroxide ((CH₃CH₂CH₂)₄NOH; TPAOH) and
80 tetraethylorthosilicate (C₈H₂₀O₄Si; TEOS) were purchased from Sigma Aldrich Co. Ltd

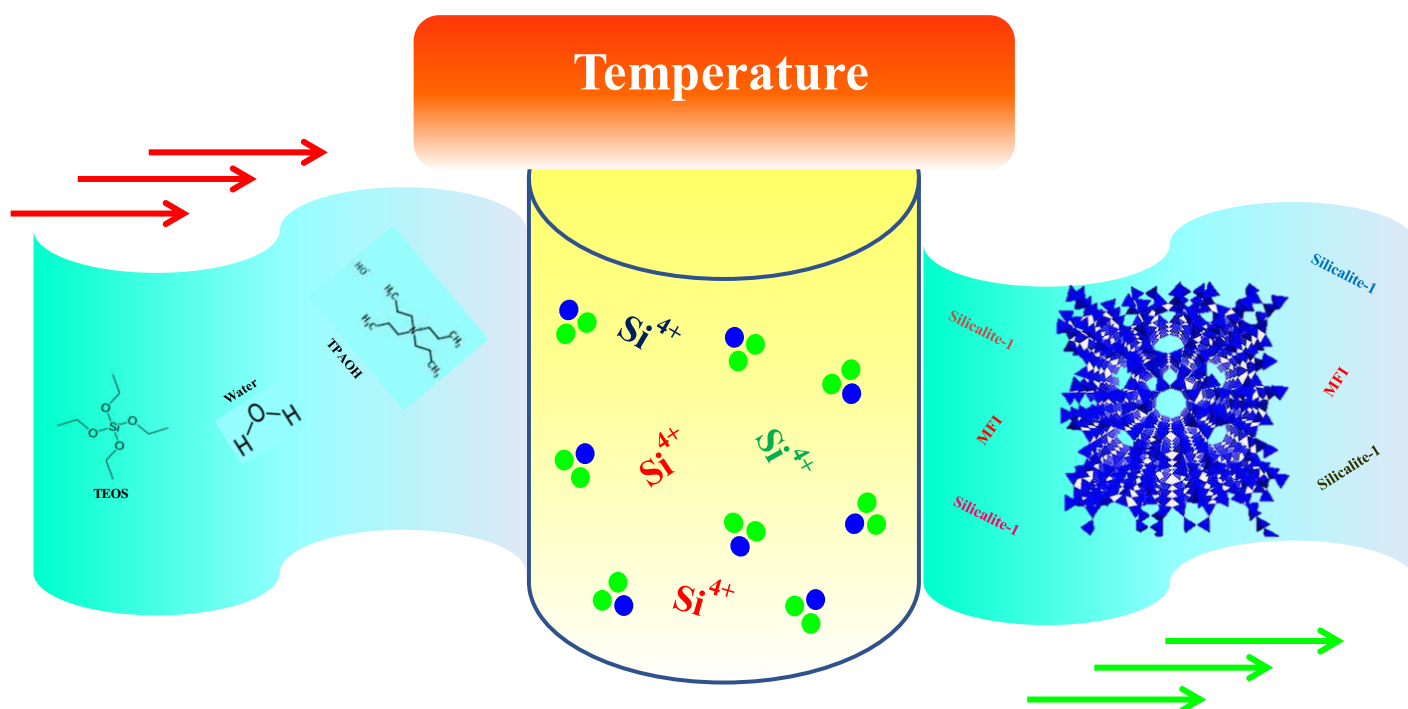
81 (India). Carboxymethyl cellulose ($[\text{C}_6\text{H}_7\text{O}_2(\text{OH})_x(\text{OCH}_2\text{COONa})_y]_n$, CMC), and methylene
82 blue ($\text{C}_{16}\text{H}_{18}\text{ClN}_3\text{S}$, MB) were purchased from Merck Co. Ltd (India). All the chemicals were
83 used as such without further purification.



91 **Figure 1.** Structural formula of methylene blue

92 **Synthesis of mesoporous silicalite-1**

94 The mesoporous silicalite-1 was synthesized by adopting hydrothermal method. In a typical
95 synthesis, 3.49 g of tetra propylammonium hydroxide (TPAOH) and 3.1 g of tetraethyl
96 orthosilicate (TEOS) were mixed in distilled water under constant stirring for 5 h. After wards,
97 0.2 g of CMC is mixed to the above solution with constant stirring. The solution was
98 concentrated in a rotavapor at 80 °C for 30 min to form a viscous solution. The resulting sol
99 was introduced into a stainless autoclave for crystallisation at 80 °C for 24 h followed by high
100 temperature treatment at 175 °C for 8 h. The obtained product was filtered, washed with water,
101 dried and finally calcined at 550 °C for 5 h to remove the organic components. For comparison
102 purpose, conventional silicalite-1 was prepared with similar procedure without adding
103 template, CMC [34, 35].



105

106 **Scheme 1.** Schematic diagram of silicalite-1107 **Characterization**

108 Powder X-ray diffraction (XRD) patterns in the range of $5\text{-}50^\circ$ were obtained with a Rigaku
 109 Miniflex 600 diffractometer using $\text{CuK}\alpha$ radiation at a scanning speed of $4^\circ/\text{min}$. The
 110 characteristic vibration bands were identified by Jasco 4700 FTIR spectrometer with KBr
 111 pellet. Scanning electron microscopic (SEM) images were recorded by using a Hitachi SU6600
 112 Variable Pressure Field Emission Scanning Electron Microscope (SEM). Transmission
 113 electron microscopic images (TEM) were taken with a JEOL JEM-2100 transmission electron
 114 microscope operated at an accelerating voltage of 200 kV. The thermal stability of the
 115 uncalcined sample was analysed by thermogravimetric (TG) analysis with Q50 instrument at a
 116 heating rate of $10^\circ\text{C}/\text{min}$ in nitrogen atmosphere. N_2 adsorption/desorption isotherm were
 117 employed to find out the surface area and pore size distributions at 77K with Micromeritics
 118 Gemini V-2380 surface area analyser. Before measurement the sample was outgassed at 573K
 119 for 3h. The Si/Al ratio of the samples was determined by electron dispersive spectroscopy
 120 (EDX) using JEOL JED-2300 instrument.

121 **Adsorption experiment**

122 For adsorption studies, stock solution of MB (100 ppm) was prepared in distilled water. 10, 20,
123 30, 40 and 50 ppm of dye solution was prepared by diluting the stock solution. The pH of the
124 dye solution was adjusted using HCl and NaOH. The effect of the environmental parameters
125 on dye removal was studied by varying adsorbent loading (0.02-0.10 wt%), dye concentration
126 (10-50 ppm), contact time (20-330 min) and temperature (30-60°C). Batch adsorption
127 experiment was employed to find out the adsorption capacity of MB onto the mesoporous
128 silicalite-1 sample. The dye uptake performance was assessed by soaking 0.10 wt% of
129 silicalite-1 in 50 mL of MB dye at different temperature. After predetermined time intervals
130 the sample was withdrawn, filtered and the solution was measured using UV-Vis
131 spectrophotometer at $\lambda_{\max} \sim 668$ nm. From the calibration curve, the concentration of dye in
132 the sample is noted. The experiments were done in triplicate and the average value is reported.
133 The percentage removal and equilibrium concentration were calculated as follows

134

135
$$q_e = \frac{(C_0 - C_e)V}{W} \quad \text{————— (1)}$$

136

137
$$R = \frac{C_0 - C_e}{C_0} \times 100(\%) \quad \text{————— (2)}$$

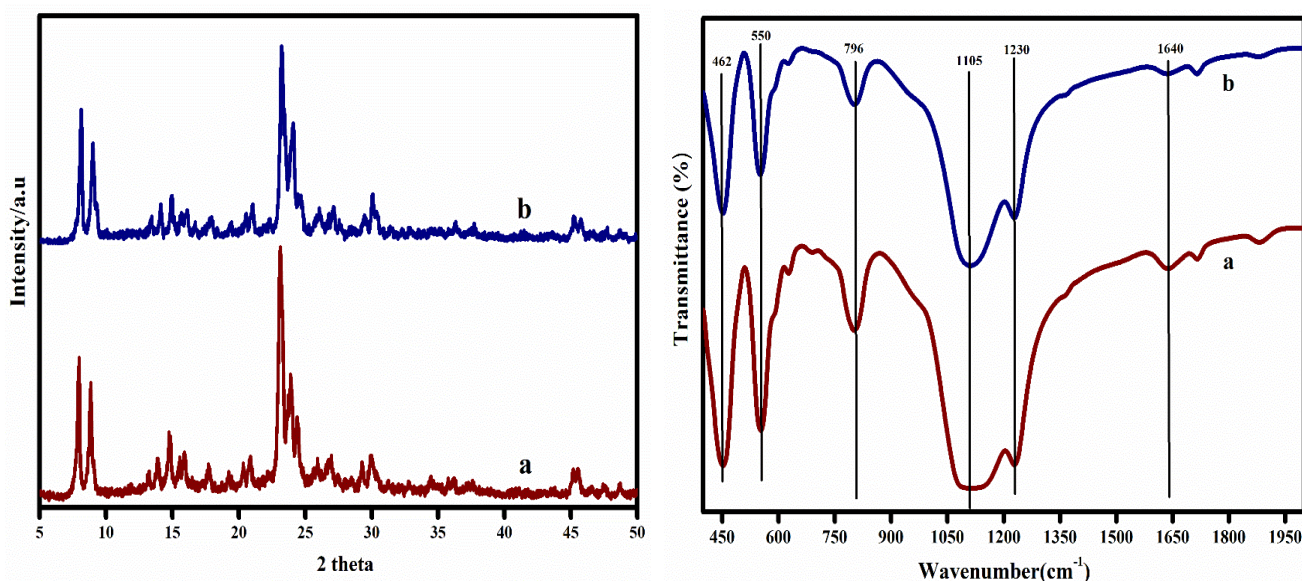
138 Where C_0 and C_e are the initial and equilibrium dye concentration (mg L^{-1}), V is the volume of
139 dye solution (L); and W is weight (g) of the adsorbent.

140 **Desorption experiment**

141 Desorption experiment of MB on silicalite-1 was performed by immersing 0.10 wt% of
142 mesoporous silicalite-1 sample in 50 mL of MB solution (10 ppm, temperature- 30°C). After
143 complete equilibrium time, the silicalite-1 was separated and eluted with 0.1 mol/L HCl to
144 desorb the dye. The silicalite-1 was later washed with distilled water, dried and used for next
145 cycle [36].

146 **Result and discussion**

147 Figure 2 shows the XRD patterns of conventional and mesoporous silicalite-1. Both silicalite-
148 1 exhibits typical MFI framework structure with five characteristic peaks at 7.98°, 8.82°, 23.18°,
149 24.02° and 24.46° corresponds to (101), (020), (503), (151) and (303) reflection respectively.
150 However, with the addition of template the peak intensity of silicalite-1 slightly reduces,
151 probably due to the development of mesopores. Thus, CMC template is efficient to generate
152 mesoporosity in silicalite-1 without compromising its crystallinity [35, 37]. To understand the
153 chemical composition of membrane, we performed FTIR spectroscopy. The FTIR spectra of
154 conventional and mesoporous silicalite-1 are displayed in Figure 3. The strong absorption band
155 at 550 cm^{-1} is attributed to double five membered ring which is characteristic of MFI
156 framework. The band at 796 cm^{-1} and 1105 cm^{-1} are assigned to Si-O-Si external symmetric
157 stretching (SiO_4 tetrahedra) and Si-O-Si internal asymmetric stretching (SiO_4 tetrahedra). The
158 band at 1230 cm^{-1} is attributed to external asymmetric stretching of Si-O bond. A weak band
159 observed at 1640 cm^{-1} could be due to the adsorbed water present in the sample. Finally, the
160 absorption band at 462 cm^{-1} is due to Si-O-Si rocking. FTIR studies were thus complimentary
161 to XRD study and confirmed the successful synthesis of silicalite-1 [33, 38].



162 **Figure 2.** Powder XRD patterns and FTIR spectra of conventional and mesoporous silicalite-
163 1

164 The morphology of conventional and mesoporous silicalite-1 was evaluated by SEM and TEM
165 analysis (Figure 3 and 4). The SEM image of mesoporous silicalite-1 (Figure 3) shows a rough
166 surface with sphere like particle in the range of 10-30 nm. The result thus suggests the
167 formation of mesopore in the system, which is attributed to the removal of templates. TEM
168 images further confirmed that mesoporous silicalite-1 have pore diameter in the range of 10-
169 30 nm. The prominent lattice fringes seen in the TEM images imply a high crystallinity for the
170 sample and are complementary to the previous reported work [39] (Figure. 4). The elemental
171 composition of mesoporous silicalite-1 is detected using EDAX measurement. The analysis
172 indicates that the synthesized sample contains only Si and O, thus confirming the product is
173 silicalite-1. N₂ adsorption/desorption isotherm were employed to characterize the surface area
174 and porosity of the sample. Figure 5(I) illustrates the N₂ adsorption/desorption isotherm of
175 conventional and mesoporous silicalite-1. As shown in Figure 5a, the conventional silicalite-1
176 belongs to type 1 isotherm with major uptake of gas at a relative low pressure ($P/P_0 < 0.2$). This
177 indicates the presence of only micropores in the system. However, mesoporous silicalite-1
178 exhibits a prominent hysteresis loop at $P/P_0 = 0.25$ to 0.9 due to the capillary condensation of
179 nitrogen. The result thus indicates the co-existence of micro and mesopores in the modified
180 sample. BJH (Barrett-Joyner-Halenda) pore size distribution is shown in Figure 5(II). It is
181 evident from figure that conventional silicalite-1 has only micropores (< 2 nm) whereas the
182 mesoporous silicalite-1 have pore diameter in the range of 10-30 nm, thus confirming the
183 presence of mesopores. This study further confirms that mesoporosity is generated in CMC
184 templated sample.

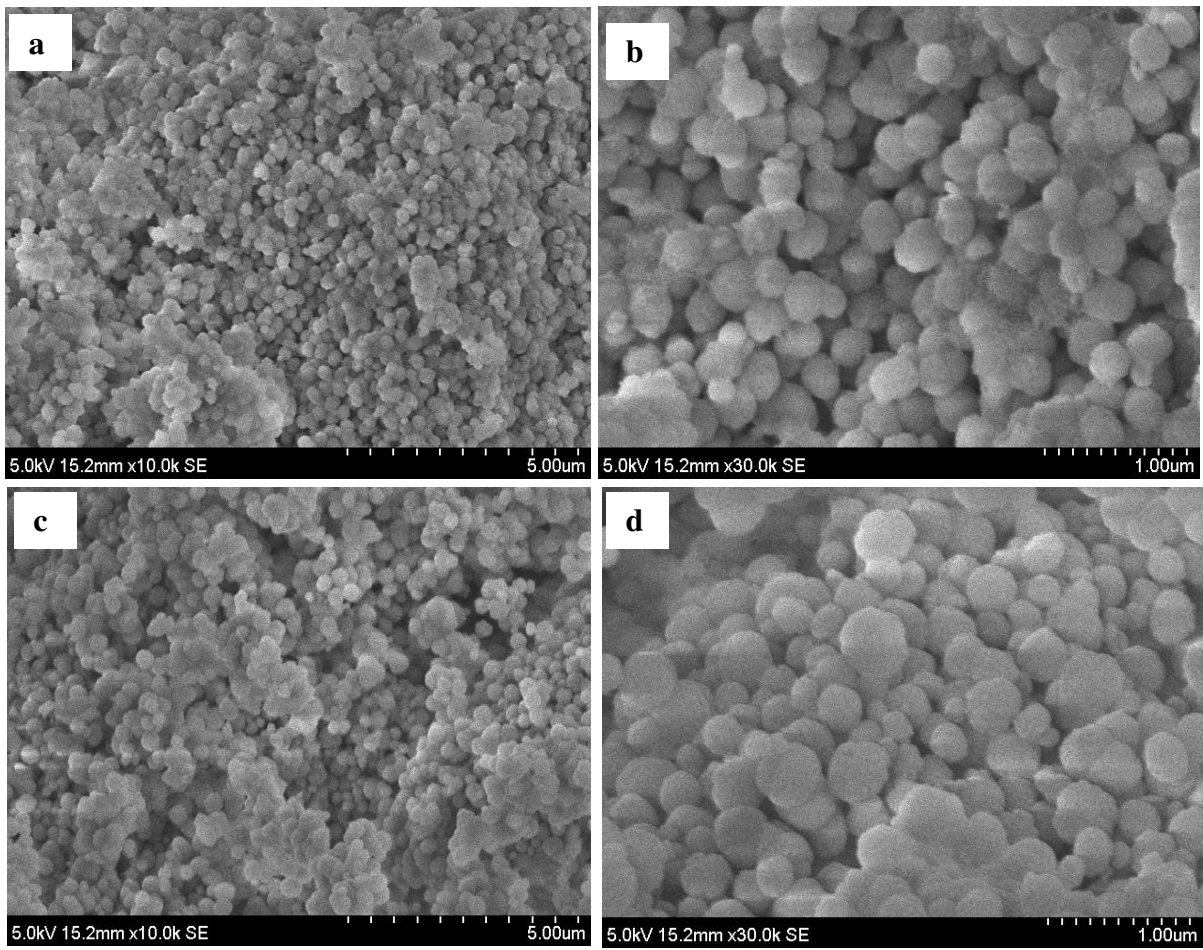
185

186

187

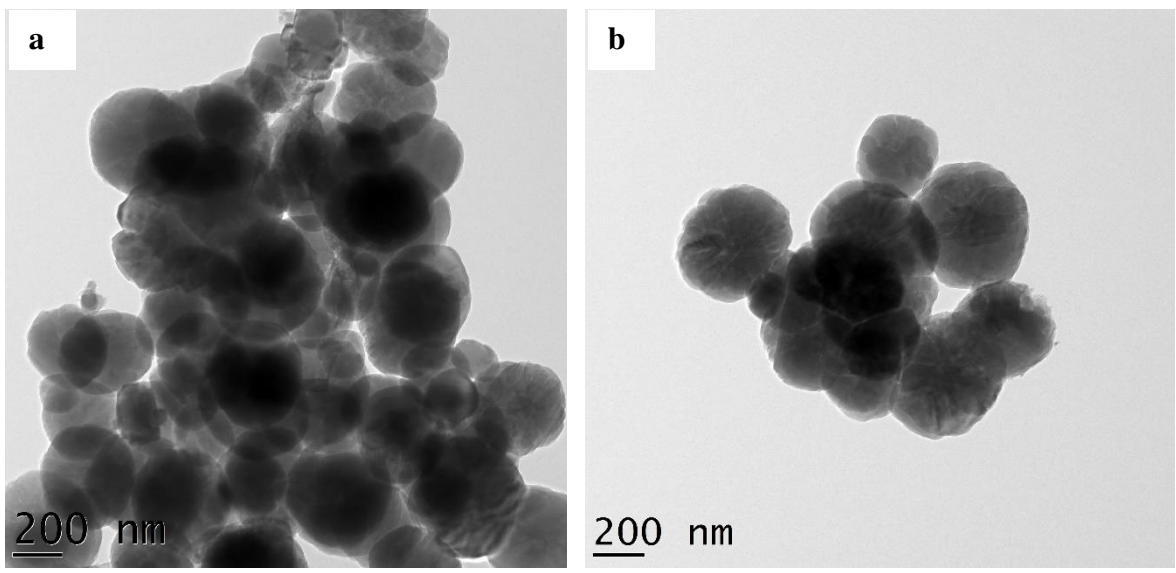
188

189
190
191
192
193
194
195
196
197
198
199
200
201
202
203
204

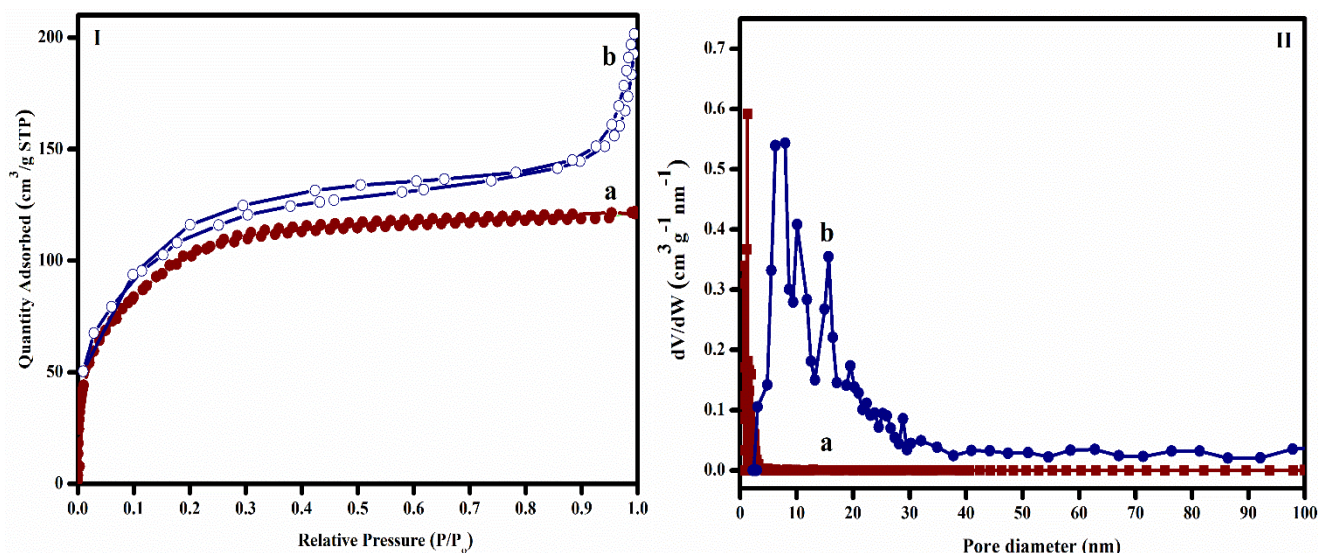


205 **Figure 3.** SEM micrographs of (a & b) conventional and (c & d) mesoporous silicalite-1

206
207
208
209
210
211
212
213
214



215
216 **Figure 4.** TEM images of mesoporous silicalite-1

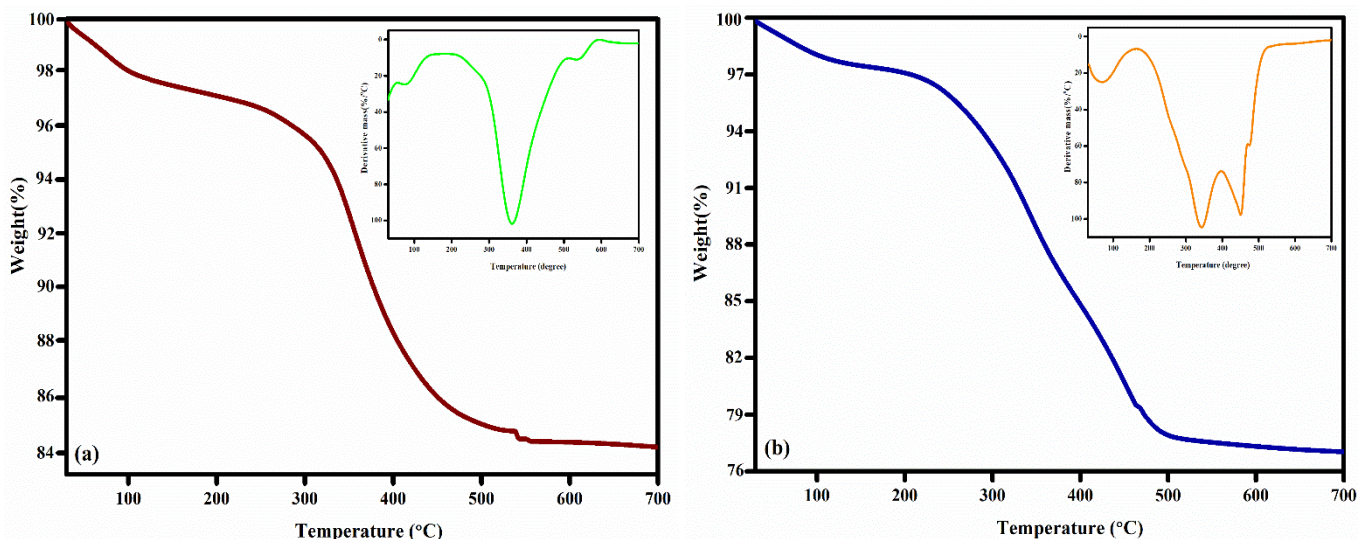


217

218 **Figure 5.** (I) N_2 adsorption isotherms of: a) conventional b) mesoporous silicalite-1; (II) pore
 219 size distribution of: a) conventional b) mesoporous silicalite-1

220 The thermal stability of conventional and mesoporous silicalite-1 is compared by
 221 thermogravimetric analysis (Figure 6). The conventional silicalite-1 showed 16% of total
 222 weight loss at 100-250°C and 300-500°C. This is attributed to the loss of water and TPAOH
 223 respectively from the silicalite-1 framework. In the case of mesopores silicalite-1, a third
 224 weight loss appears at 500°C which is due to the decomposition of template. As modified
 225 silicate possess higher weight loss (22%) than conventional silicalite-1, it is thermally more
 226 stable than conventional silicalite-1.

227



228 **Figure 6.** TGA curves of conventional and mesoporous silicalite-1 and the corresponding DTG
 229 curves are given at the inset

230

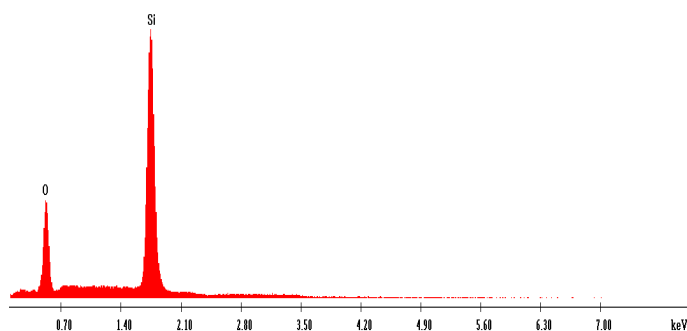
231

232

233

234

235



236

237 **Figure 7.** EDS image of mesoporous silicalite-1

238

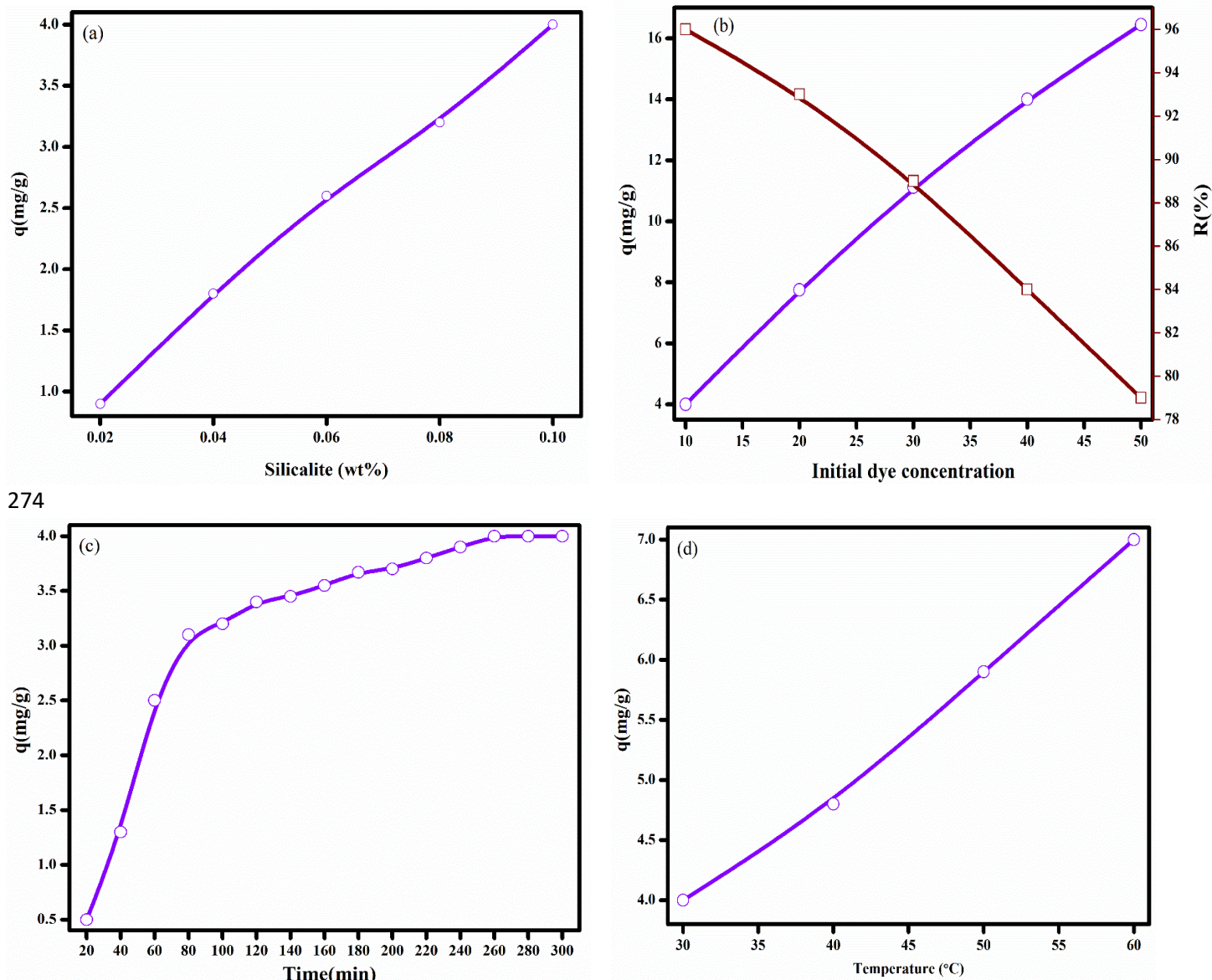
239 **Adsorption experiment of mesoporous silicalite-1 on methylene blue**

240 Due to the presence of micro and mesoporous structure, modified silicalite-1 is expected to
 241 have good adsorption capacity for dye molecule. This prompted us to monitored the dye (MB)
 242 uptake ability of modified silicate. The influence of environmental parameters such as
 243 silicalite-1 dosage, temperature, initial dye concentration and contact time was also
 244 investigated in detail. The influence of silicate dosage on the MB removal was carried out by
 245 varying the silicalite-1 from 0.02 to 0.10 wt%. From Figure 8(a), it can clearly see that the dye
 246 adsorption capacity increases linearly with adsorbent dosage. High surface area along with the

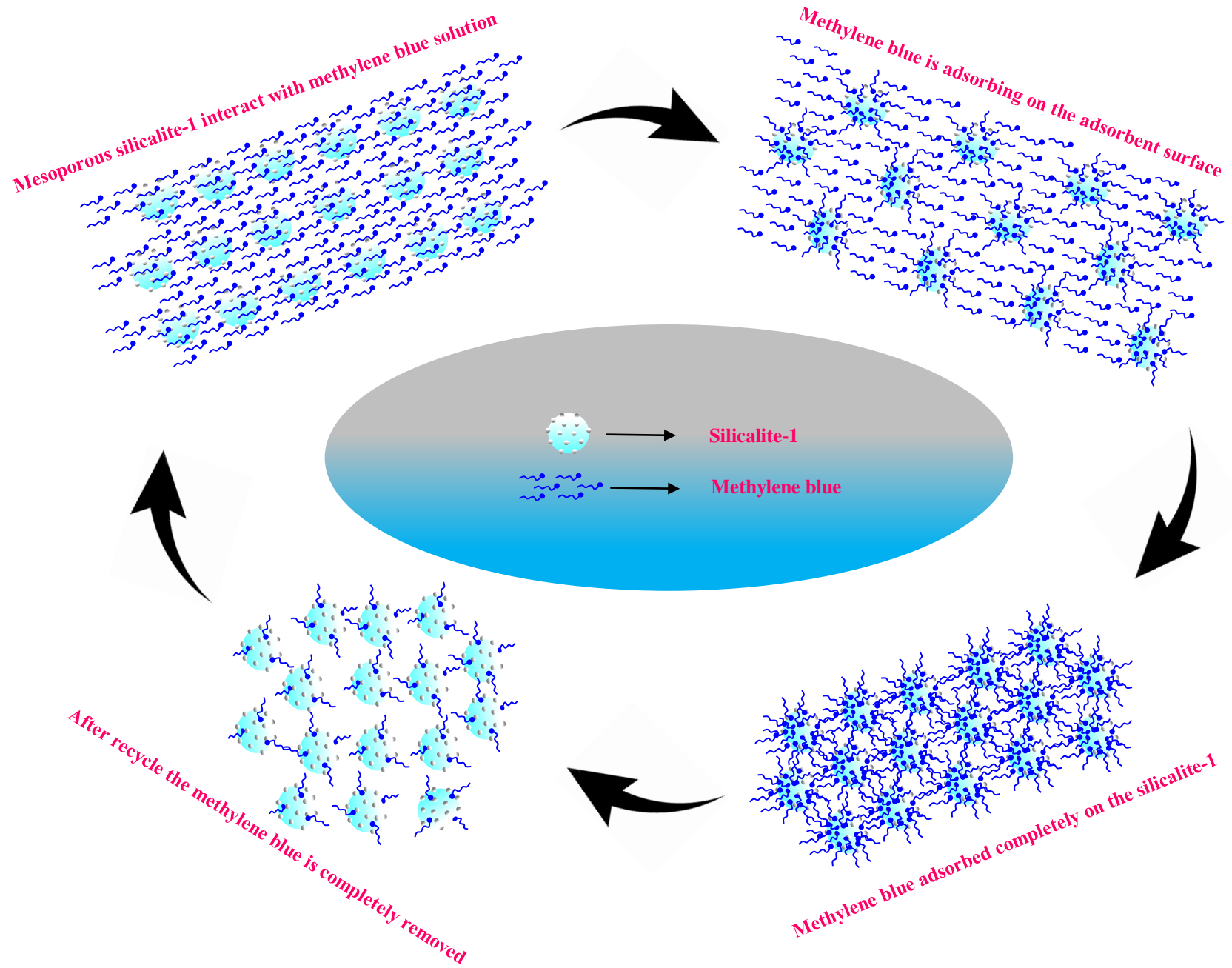
247 presence of micro/mesoporous structure on silicalite-1 could have increases the affinity of dye
248 molecule to the adsorbent. Consequently, adsorption capacity increases and a maximum
249 adsorption capacity (4 mg/g) was achieved at 0.10 wt% of adsorption dosage. The relationship
250 between initial dye concentration and adsorption capacity of MB is shown in Figure 8(b). It is
251 evident from figure that when the initial dye concentration increases from 10 to 50 ppm, the
252 adsorption capacity increases from 4 to 16.45 mg/g. Similar results have also been reported by
253 Duman et al [40]. They observed that on increasing the initial dye concentration from 20 to 40
254 mg/L the adsorption capacity increases from 8 to 15 mg/g. Dong et al. [41] reported that
255 mesoporous SBA-15 exhibits high adsorption capacity when the initial concentration exceeds
256 230 mg/g. According to the authors high initial concentration provides a necessary driving
257 force for the diffusion of dye from aqueous to the solid phase. We have varied the immersing
258 time from 10-330 min and evaluate its effect on the MB adsorption was in the following
259 operational conditions initial dye concentration -10ppm, temperature-30°C and dosage-0.1
260 wt%. In the initial contact time, due to availability of large number of unoccupied active sites
261 on the surface of adsorbent, the rate of adsorption increases, Therefore, adsorption capacity
262 steeply rises in the initial phase of contact time. However, the rate of adsorption becomes
263 gradual 120 min and eventually at 240 min it reaches constant. This implies that the adsorption
264 site on the surface of silicalite-1 get saturated with contact time and after 240 min complete
265 occupation of adsorption site happens. Similar curve was noted by Mouni et al. they obtained
266 equilibrium at 120 min [42]. Figure 8(d) show the adsorption capacity at different temperature
267 (30 to 60°C). On increasing the temperature from 30 to 60°C, the adsorption capacity increases
268 from 4 to 7 mg/g, thus suggesting that the MB adsorption on silicalite-1 is endothermic. High
269 temperature tends to enhances the mobility of dye molecule. As a result, the dye molecule can
270 easily diffuse from the solution phase to the adsorbent phase. Therefore, high temperature

271 favours the MB adsorption on silicalite-1. Scheme 2 show the schematic representation of
272 mesoporous silicalite-1 will interact with MB dye molecule.

273



275 **Figure 8.** Effect of various parameters on the adsorption of MB onto mesoporous silicalite-1
276 a) silicalite-1 dosage b) initial dye concentration c) contact time d) temperature on the
277 adsorption process (adsorbent dosage = 0.10 wt%, initial MO concentration = 10 ppm, contact
278 time = 240 min and temperature= 30°C



Scheme 2. Mechanism for MB adsorption on mesoporous silicalite-1

1 Adsorption kinetics

2 Adsorption kinetics was investigated to understand the adsorption mechanism and rate of
3 adsorption of MB dye onto adsorbent. The experimental data was evaluated using two well-
4 known models; pseudo-first-order and pseudo-second-order model. The linearized form of
5 pseudo-first-order kinetic equation is expressed as follows [43]

$$6 \quad \log(q_e - q_t) = \log q_e - \frac{K_1 t}{2.303} \quad (3)$$

7 where q_t (mg/g) and q_e (mg/g) are the amount of dye adsorbed at time 't' and equilibrium. K_1
8 are pseudo-first-order rate constant in 1/min. The graph of $\log (q_e - q_t)$ vs. t gives a straight
9 with k_1 as slope and q_e as intercept.

10 The pseudo-second-order model is as follow[44]

$$11 \quad \frac{t}{q_e} = \frac{1}{K_2 q_e^2} + \frac{t}{q_e} \quad (4)$$

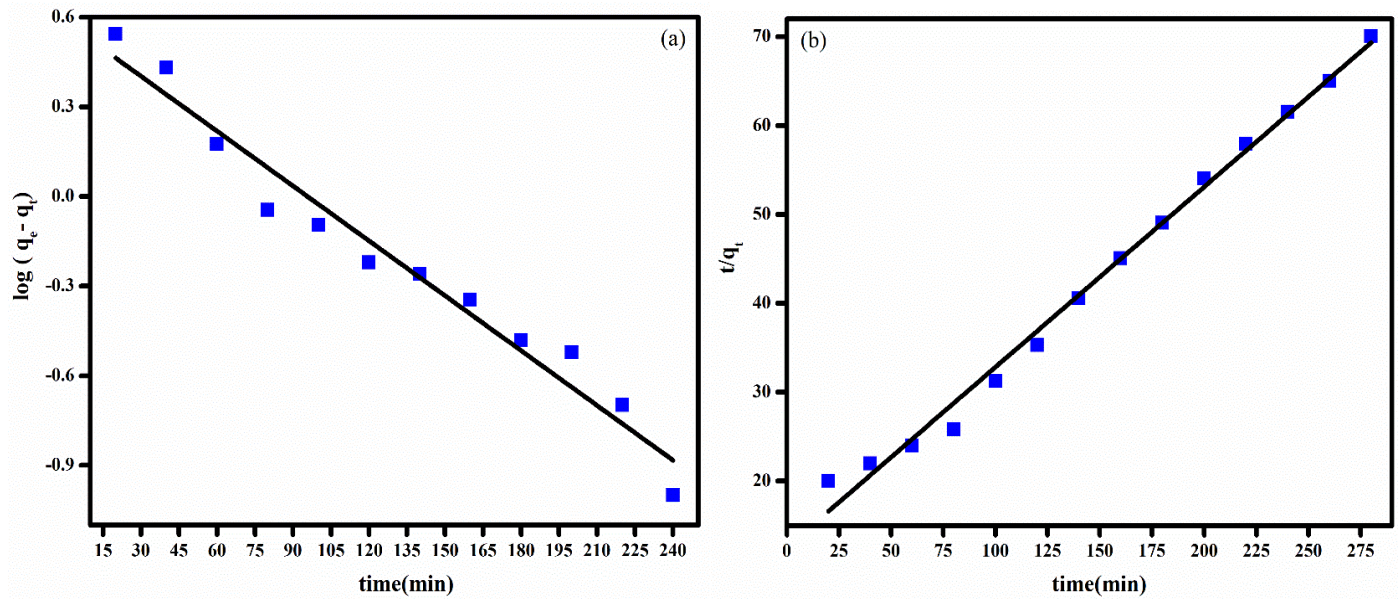
12 where K_2 is pseudo-second-order rate constant (g/mg min) and q_e is equilibrium adsorption
13 capacity. The value of q_e and K_2 were obtained from the slope and intercept of plot t/q_t vs t.

14 The experimental data fitting on the kinetic model is illustrated in Figure 9 and the
15 corresponding kinetic data are presented in Table 1. the validity of these models was checked
16 by noting the correlation coefficient value (R^2). As can be seen, the experimental value fitted
17 well in pseudo-second-order (0.99) model than pseudo-first-order (0.95). In addition to this,
18 the correlation coefficient of pseudo-second-order model is higher than pseudo-first-order
19 model. Therefore, pseudo-second-order is more suitable than pseudo-first order to explain
20 kinetics of MB uptake on silicalite-1.

21

22

23



24
 25 **Figure 9.** a) pseudo-first-order b) pseudo-second-order models for the adsorption of MB dye
 26 onto mesoporous silicalite-1
 27

28 **Table 1.** Kinetic parameter values of adsorption kinetics for MB onto mesoporous silicalite-1

Experimental		PFO		PSO		
$q_e, \text{exp (mg g}^{-1}\text{)}$	$K_1(\text{min}^{-1})$	$q_e \text{ (mg g}^{-1}\text{)}$	R^2	$K_2(\text{g mg}^{-1} \text{min}^{-1})$	$q_e(\text{mg g}^{-1})$	R^2
4	-0.0140	3.2	0.95	0.0031	3.95	0.99

29
 30 **Adsorption isotherm**
 31 Adsorption isotherm is essential to understand the adsorption behaviour and interaction
 32 between the adsorbate and adsorbent. The linear form of Langmuir model is expressed as
 33 follows[45, 46]

34
$$\frac{C_e}{q_e} = \frac{C_e}{q_{\max}} + \frac{1}{K_L q_{\max}} \quad (5)$$

35 where q_e is the amount of MB dye adsorbed at equilibrium, C_e is the equilibrium concentration
 36 of MB dye (mg/L), q_{\max} is maximum adsorption capacity, K_L and R_L are characteristic
 37 Langmuir parameters which is termed as Langmuir adsorption constant and separation factor
 38 respectively. R_L is expressed as

39
$$R_L = \frac{1}{1 + K_L C_0} \quad (6)$$

40

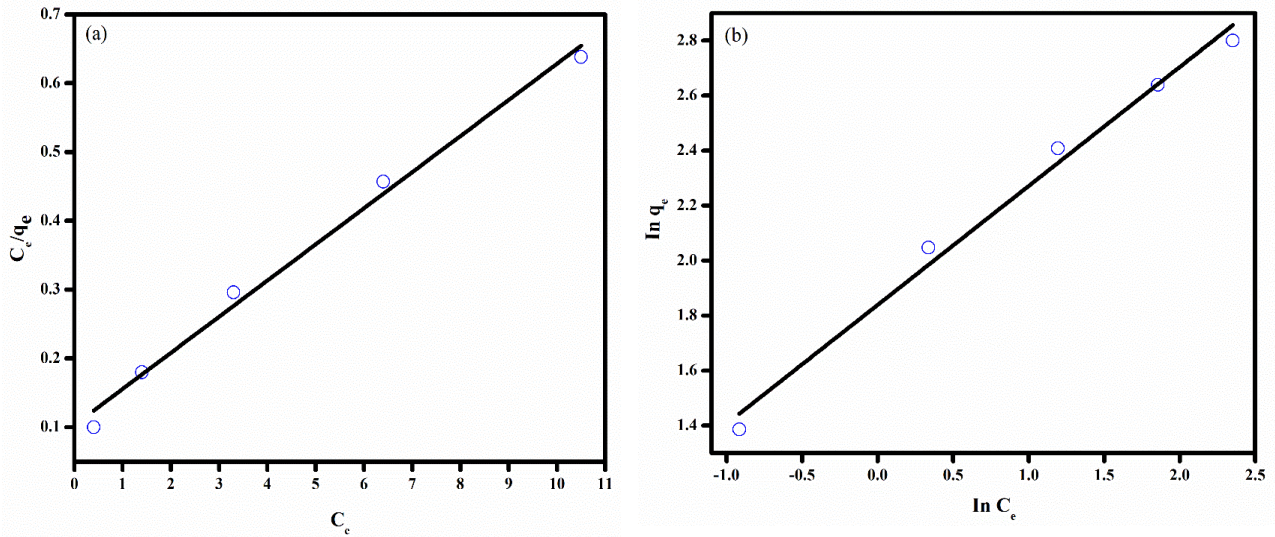
41 Here, C_0 is initial MB concentration (mg/L). The value of R_L is significant and is related to the
 42 feasibility of adsorption. The adsorption process is favorable, if R_L is between 0 and 1,
 43 unfavorable if $R_L > 1$. $R_L=0$ and $R_L=1$ indicates reversible and linear adsorption respectively
 44 [52].

45 The Langmuir isotherm model assumes a homogeneous surface with equivalent site. According
 46 to this model, there is no interaction between the adsorbed molecules and hence multilayer
 47 adsorption will not occur. From the linear plot of C_e/q_e vs. C_e , the value of q_e and K_L is obtained.
 48 The Freundlich isotherm on the other hand assume heterogeneous surface and there is no
 49 restriction of multilayer formation. Therefore, in this model both monolayer and multilayer
 50 adsorption can take place. The linearized form of Freundlich model is represented as [47]

51
$$\ln q_e = \frac{1}{n} \ln C_e + \ln K_F \quad (7)$$

52 Where K_F and n are Freundlich constants related to adsorption capacity and degree of
 53 adsorption respectively. The value of K_F and n can be determined from the plot of $\ln q_e$ vs. \ln
 54 C_e .

55 The data of adsorption process were applied to Langmuir and Freundlich isotherm model and
 56 the adsorption parameters are shown in Table 2. Since Freundlich isotherm gives a better fit
 57 with high correlation coefficient (R^2) it could be more suitable for MB adsorption. The value
 58 of $1/n$ is between 0 and 1 indicating that the MB adsorption on mesoporous silicalite-1 is a
 59 favourable process.



60 **Figure 10.** Isotherm model plots for the adsorption of MB a) Langmuir isotherm b) Freundlich
 61 isotherm

62

63 **Table 2.** Langmuir isotherm and Freundlich isotherm parameter values for MB adsorption onto
 64 mesoporous silicalite-1

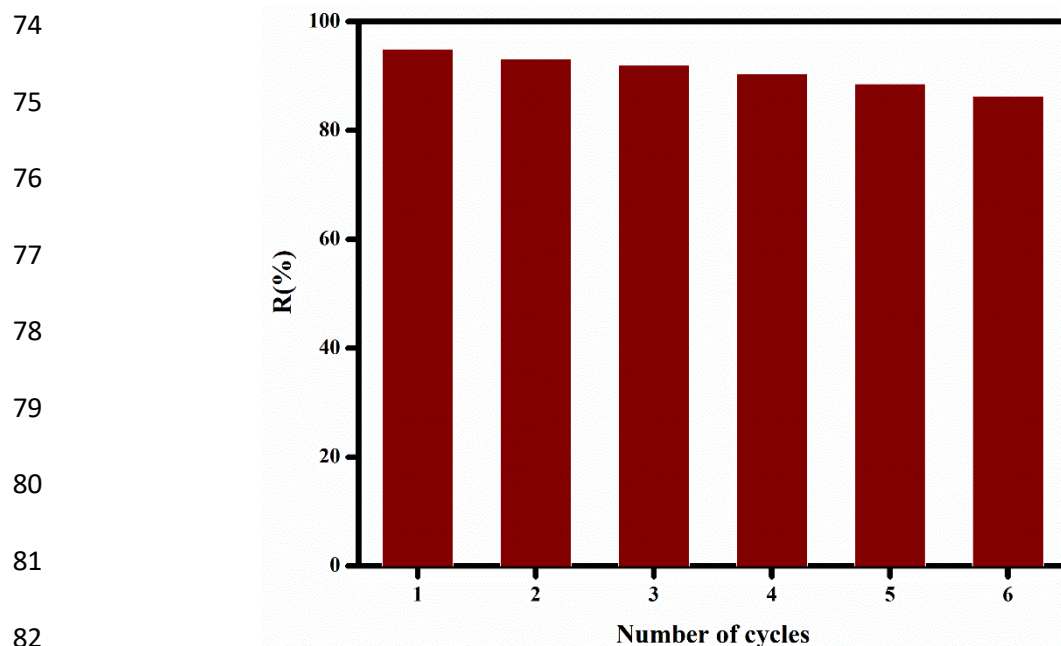
Experimental		Langmuir isotherm		Freundlich isotherm		
$q_e, \text{exp (mg g}^{-1}\text{)}$	R^2	$q_{\text{max}}(\text{mg g}^{-1})$	K_L	R^2	$K_F(\text{mg g}^{-1})$	n
4	0.977	19.04	0.509	0.995	4.3	2.31

65

66 **Recyclability**

67 The regeneration performance of the modified silicalite-1 was studied by six
 68 adsorption–desorption cycles at fixed adsorbent dose of 0.10 wt% and initial dye concentration
 69 10 ppm. The result is presented in Figure 11. The result shows that the removal percentage of
 70 membrane at the first adsorption–desorption cycle is 95% and after six adsorption–desorption
 71 cycles, the adsorption efficiency was reduced to 86.3%. The results thus demonstrate that the
 72 silicalite-1 is effective even after multiple reuses.

73



83 **Figure 11.** Reusability performance of adsorption of MB onto mesoporous silicalite-1

84 **Conclusion**

85 In the present study, a mesoporous silicalite-1 was developed using eco-friendly template,
 86 CMC. The successful synthesis of modified silicate was confirmed by techniques such as SEM,
 87 TEM, N₂ isotherm, XRD, FTIR. The synthesized mesoporous silicalite-1 was effective to
 88 remove the cationic dye methylene blue from water. The effect of various operational
 89 parameter on the dye adsorption was studied and the result indicate that adsorption is favored
 90 at high initial concentration, high immersing time and high temperature. The dye removal was
 91 found to be governed by Freundlich isotherm model and the rate of adsorption was found to
 92 obey pseudo-second-order kinetics. The mesoporous silicalite-1 sample also show excellent
 93 recyclability. Therefore, we can conclude that modified silicalite-1 is a highly attractive
 94 candidate for the removal of MB from water.

95 **Consent for publication**

96 The authors confirm the consent for publication

97 **Availability of data and material**

98 All data generated or analysed during this study are included in this published article

99

100 **Funding**

101 (Grant No. KMUTNB-63-Post-03 to SR) and (Grant No. KMUTNB-64-03, KMUTNB-
102 BasicR-64-16)

103 **Authors contribution**

104 Sabarish Radoor- Conceptualization, Methodology, Investigation, Validation, Writing -
105 original draft, Software, Writing - review & editing, Formal analysis; Jasila Karayil -
106 Investigation, Analysis, Interpretation of results, Software, Writing – review & editing, Formal
107 analysis.; Aswathy Jayakumar - Data collection, Validation, Writing - review & editing,
108 Formal analysis; Jyothi Mannekote Shivanna - Interpretation of results, Software, Writing –
109 review & editing, Jyotishkumar Parameswaranpillai –Validation, Software, Writing - review
110 & editing and Investigation; Suchart Siengchin – Editing, Funding and Supervision

111 **Acknowledgements**

112 The study was financially supported by the King Mongkut's University of Technology North
113 Bangkok (KMUTNB), Thailand through the Post-Doctoral Program (Grant No. KMUTNB-
114 63-Post-03 and KMUTNB-64-Post-03 to SR) and (Grant No. KMUTNB-BasicR-64-16)

115 **Compliance with ethical standards**

116 **Conflict of interest:** The authors have declared no conflict of interest

117 **References**

- 118 [1] S. Wang, E. Ariyanto, Competitive adsorption of malachite green and Pb ions on natural zeolite,
119 Journal of Colloid and Interface Science, 314 (2007) 25-31.
120 [2] X.S. Wang, Y. Zhou, Y. Jiang, C. Sun, The removal of basic dyes from aqueous solutions using
121 agricultural by-products, Journal of Hazardous Materials, 157 (2008) 374-385.
122 [3] S. Radoor, J. Karayil, J. Parameswaranpillai, S. Siengchin, Removal of anionic dye Congo red from
123 aqueous environment using polyvinyl alcohol/sodium alginate/ZSM-5 zeolite membrane, Scientific
124 Reports, 10 (2020).
125 [4] V.K. Gupta, Suhas, Application of low-cost adsorbents for dye removal – A review, Journal of
126 Environmental Management, 90 (2009) 2313-2342.
127 [5] R. Sabarish, G. Unnikrishnan, Polyvinyl alcohol/carboxymethyl cellulose/ZSM-5 zeolite
128 biocomposite membranes for dye adsorption applications, Carbohydrate Polymers, 199 (2018) 129-
129 140.

130 [6] R. Sabarish, G. Unnikrishnan, PVA/PDADMAC/ZSM-5 zeolite hybrid matrix membranes for dye
131 adsorption: Fabrication, characterization, adsorption, kinetics and antimicrobial properties, *Journal*
132 *of Environmental Chemical Engineering*, 6 (2018) 3860-3873.

133 [7] E. Forgacs, T. Cserháti, G. Oros, Removal of synthetic dyes from wastewaters: a review,
134 *Environment International*, 30 (2004) 953-971.

135 [8] H. Ali, Biodegradation of Synthetic Dyes—A Review, *Water, Air, & Soil Pollution*, 213 (2010) 251-
136 273.

137 [9] S. Radoor, J. Karayil, J. Parameswaranpillai, S. Siengchin, Adsorption Study of Anionic Dye,
138 Eriochrome Black T from Aqueous Medium Using Polyvinyl Alcohol/Starch/ZSM-5 Zeolite Membrane,
139 *Journal of Polymers and the Environment*, 28 (2020) 2631-2643.

140 [10] S. Mahdavi, M. Jalali, A. Afkhami, Removal of heavy metals from aqueous solutions using Fe₃O₄,
141 ZnO, and CuO nanoparticles, in: *Nanotechnology for Sustainable Development*, 2012, pp. 171-188.

142 [11] A.G. El-Shamy, An efficient removal of methylene blue dye by adsorption onto carbon dot @
143 zinc peroxide embedded poly vinyl alcohol (PVA/CZnO₂) nano-composite: A novel Reusable
144 adsorbent, *Polymer*, 202 (2020).

145 [12] K.-T. Chung, Azo dyes and human health: A review, *Journal of Environmental Science and*
146 *Health, Part C*, 34 (2016) 233-261.

147 [13] S. Mani, P. Chowdhary, R.N. Bharagava, Textile Wastewater Dyes: Toxicity Profile and Treatment
148 Approaches, in: *Emerging and Eco-Friendly Approaches for Waste Management*, 2019, pp. 219-244.

149 [14] M. Rafatullah, O. Sulaiman, R. Hashim, A. Ahmad, Adsorption of methylene blue on low-cost
150 adsorbents: A review, *Journal of Hazardous Materials*, 177 (2010) 70-80.

151 [15] L. Shi, L. Hu, J. Zheng, M. Zhang, J. Xu, Adsorptive Removal of Methylene Blue from Aqueous
152 Solution using a Ni-Metal Organic Framework Material, *Journal of Dispersion Science and*
153 *Technology*, 37 (2015) 1226-1231.

154 [16] A. Kumar, H.M. Jena, Removal of methylene blue and phenol onto prepared activated carbon
155 from Fox nutshell by chemical activation in batch and fixed-bed column, *Journal of Cleaner*
156 *Production*, 137 (2016) 1246-1259.

157 [17] S. Kumari, G.S. Chauhan, J.H. Ahn, Novel cellulose nanowhiskers-based polyurethane foam for
158 rapid and persistent removal of methylene blue from its aqueous solutions, *Chemical Engineering*
159 *Journal*, 304 (2016) 728-736.

160 [18] N. Mallick, *BioMetals*, 15 (2002) 377-390.

161 [19] M. Bayat, V. Javanbakht, J. Esmaili, Synthesis of zeolite/nickel ferrite/sodium alginate
162 bionanocomposite via a co-precipitation technique for efficient removal of water-soluble methylene
163 blue dye, *International Journal of Biological Macromolecules*, 116 (2018) 607-619.

164 [20] E. Alver, A.Ü. Metin, Anionic dye removal from aqueous solutions using modified zeolite:
165 Adsorption kinetics and isotherm studies, *Chemical Engineering Journal*, 200-202 (2012) 59-67.

166 [21] M. Anbia, S. Salehi, Removal of acid dyes from aqueous media by adsorption onto amino-
167 functionalized nanoporous silica SBA-3, *Dyes and Pigments*, 94 (2012) 1-9.

168 [22] G.V. Brião, S.L. Jahn, E.L. Foletto, G.L. Dotto, Adsorption of crystal violet dye onto a mesoporous
169 ZSM-5 zeolite synthesized using chitin as template, *Journal of Colloid and Interface Science*, 508
170 (2017) 313-322.

171 [23] H. Aysan, S. Edebali, C. Ozdemir, M. Celik Karakaya, N. Karakaya, Use of chabazite, a naturally
172 abundant zeolite, for the investigation of the adsorption kinetics and mechanism of methylene blue
173 dye, *Microporous and Mesoporous Materials*, 235 (2016) 78-86.

174 [24] A.H. Jawad, A.S. Abdulhameed, Mesoporous Iraqi red kaolin clay as an efficient adsorbent for
175 methylene blue dye: Adsorption kinetic, isotherm and mechanism study, *Surfaces and Interfaces*, 18
176 (2020).

177 [25] I. Chaari, E. Fakhfakh, M. Medhioub, F. Jamoussi, Comparative study on adsorption of cationic
178 and anionic dyes by smectite rich natural clays, *Journal of Molecular Structure*, 1179 (2019) 672-677.

179 [26] B.K. Preetha, B. Vishalakshi, Microwave assisted synthesis of karaya gum based montmorillonite
180 nanocomposite: Characterisation, swelling and dye adsorption studies, *International Journal of*
181 *Biological Macromolecules*, 154 (2020) 739-750.

182 [27] M.A. Ahmad, M.A. Eusoff, P.O. Oladoye, K.A. Adegoke, O.S. Bello, Statistical optimization of
183 Remazol Brilliant Blue R dye adsorption onto activated carbon prepared from pomegranate fruit
184 peel, *Chemical Data Collections*, 28 (2020).

185 [28] N.M. Mahmoodi, M. Taghizadeh, A. Taghizadeh, Mesoporous activated carbons of low-cost
186 agricultural bio-wastes with high adsorption capacity: Preparation and artificial neural network
187 modeling of dye removal from single and multicomponent (binary and ternary) systems, *Journal of*
188 *Molecular Liquids*, 269 (2018) 217-228.

189 [29] C. Yin, J. He, S. Liu, Synthesis of mesoporous silicalite-1 zeolite for the vapor phase Beckmann
190 rearrangement of cyclohexanone oxime, *Microporous and Mesoporous Materials*, 307 (2020).

191 [30] J. Yang, Y.-X. Huang, Y. Pan, J.-X. Mi, Green synthesis and characterization of zeolite silicalite-1
192 from recycled mother liquor, *Microporous and Mesoporous Materials*, 303 (2020).

193 [31] Y.Q. Jing, Y.C. Wang, Y.Z. Gao, H.Q. Li, Y.Y. Cheng, P. Lu, Y.H. Zhang, C. Ma, Synthesis of TiO₂-
194 loaded silicate-1 monoliths and their application for degradation rhodamine B, *RSC Advances*, 6
195 (2016) 42495-42501.

196 [32] Z.-L. Cheng, Y.-x. Li, Z. Liu, Fabrication of graphene oxide/silicalite-1 composites with hierarchical
197 porous structure and investigation on their adsorption performance for rhodamine B, *Journal of*
198 *Industrial and Engineering Chemistry*, 55 (2017) 234-243.

199 [33] R. Sabarish, G. Unnikrishnan, Novel biopolymer templated hierarchical silicalite-1 as an
200 adsorbent for the removal of rhodamine B, *Journal of Molecular Liquids*, 272 (2018) 919-929.

201 [34] R. Sabarish, G. Unnikrishnan, Synthesis, characterization and catalytic activity of hierarchical
202 ZSM-5 templated by carboxymethyl cellulose, *Powder Technology*, 320 (2017) 412-419.

203 [35] R. Sabarish, G. Unnikrishnan, Synthesis, characterization and evaluations of micro/mesoporous
204 ZSM-5 zeolite using starch as bio template, *SN Applied Sciences*, 1 (2019).

205 [36] T. Huang, M. Yan, K. He, Z. Huang, G. Zeng, A. Chen, M. Peng, H. Li, L. Yuan, G. Chen, Efficient
206 removal of methylene blue from aqueous solutions using magnetic graphene oxide modified zeolite,
207 *Journal of Colloid and Interface Science*, 543 (2019) 43-51.

208 [37] R. Ling, W. Chen, J. Hou, Preparation of modified MFI (ZSM-5 and silicalite-1) zeolites for
209 potassium extraction from seawater, *Particuology*, 36 (2018) 190-192.

210 [38] H. Yang, P. Yang, X. Liu, Y. Wang, Space-confined synthesis of zeolite Beta microspheres via
211 steam-assisted crystallization, *Chemical Engineering Journal*, 299 (2016) 112-119.

212 [39] B. Wang, T. Guo, Y. Zhang, F. Chen, P. Rui, X. Xie, W. Liao, Y. Luo, X. Shu, Cobalt oxide
213 encapsulated hydrophilic hierarchical Silicalite-1 for highly efficient conversion of cyclohexyl
214 hydroperoxide, *Microporous and Mesoporous Materials*, 302 (2020).

215 [40] O. Duman, T.G. Polat, C.Ö. Diker, S. Tunç, Agar/κ-carrageenan composite hydrogel adsorbent for
216 the removal of Methylene Blue from water, *International Journal of Biological Macromolecules*, 160
217 (2020) 823-835.

218 [41] Y. Dong, B. Lu, S. Zang, J. Zhao, X. Wang, Q. Cai, Removal of methylene blue from coloured
219 effluents by adsorption onto SBA-15, *Journal of Chemical Technology & Biotechnology*, 86 (2011)
220 616-619.

221 [42] L. Mouni, L. Belkhir, J.-C. Bollinger, A. Bouzaza, A. Assadi, A. Tirri, F. Dahmoune, K. Madani, H.
222 Remini, Removal of Methylene Blue from aqueous solutions by adsorption on Kaolin: Kinetic and
223 equilibrium studies, *Applied Clay Science*, 153 (2018) 38-45.

224 [43] G. Limousin, J.P. Gaudet, L. Charlet, S. Szenknect, V. Barthès, M. Krimissa, Sorption isotherms: A
225 review on physical bases, modeling and measurement, *Applied Geochemistry*, 22 (2007) 249-275.

226 [44] Y. Ho, Review of second-order models for adsorption systems, *Journal of Hazardous Materials*,
227 136 (2006) 681-689.

228 [45] D. Mohan, K.P. Singh, G. Singh, K. Kumar, Removal of Dyes from Wastewater Using Flyash, a
229 Low-Cost Adsorbent†, *Industrial & Engineering Chemistry Research*, 41 (2002) 3688-3695.

230 [46] A. Afkhami, R. Moosavi, Adsorptive removal of Congo red, a carcinogenic textile dye, from
231 aqueous solutions by maghemite nanoparticles, *Journal of Hazardous Materials*, 174 (2010) 398-403.
232 [47] A.S. Eltaweil, H. Ali Mohamed, E.M. Abd El-Monaem, G.M. El-Subruiti, Mesoporous magnetic
233 biochar composite for enhanced adsorption of malachite green dye: Characterization, adsorption
234 kinetics, thermodynamics and isotherms, *Advanced Powder Technology*, 31 (2020) 1253-1263.

235

Figures

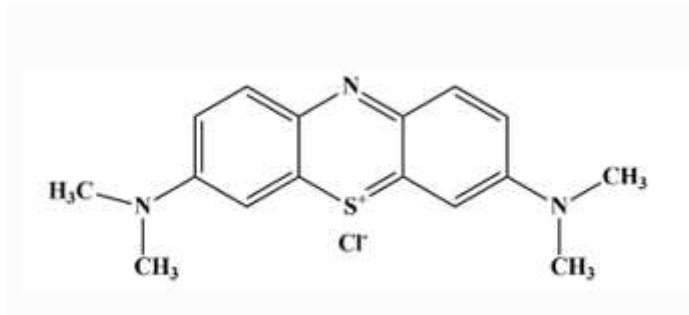


Figure 1

Structural formula of methylene blue

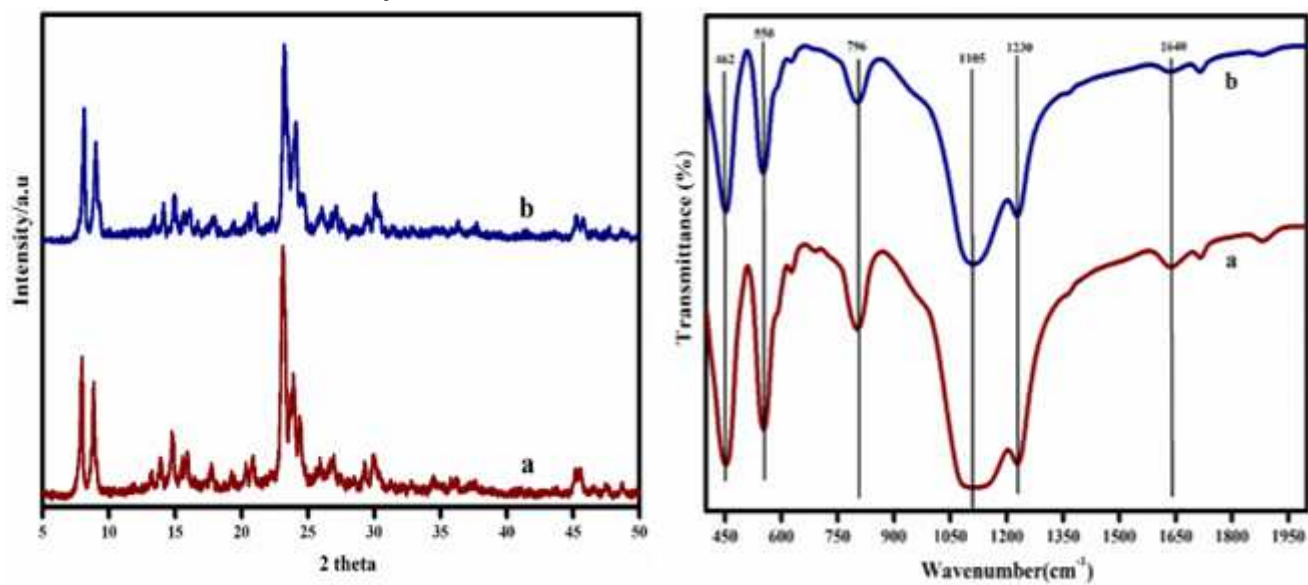


Figure 2

Powder XRD patterns and FTIR spectra of conventional and mesoporous silicalite-1

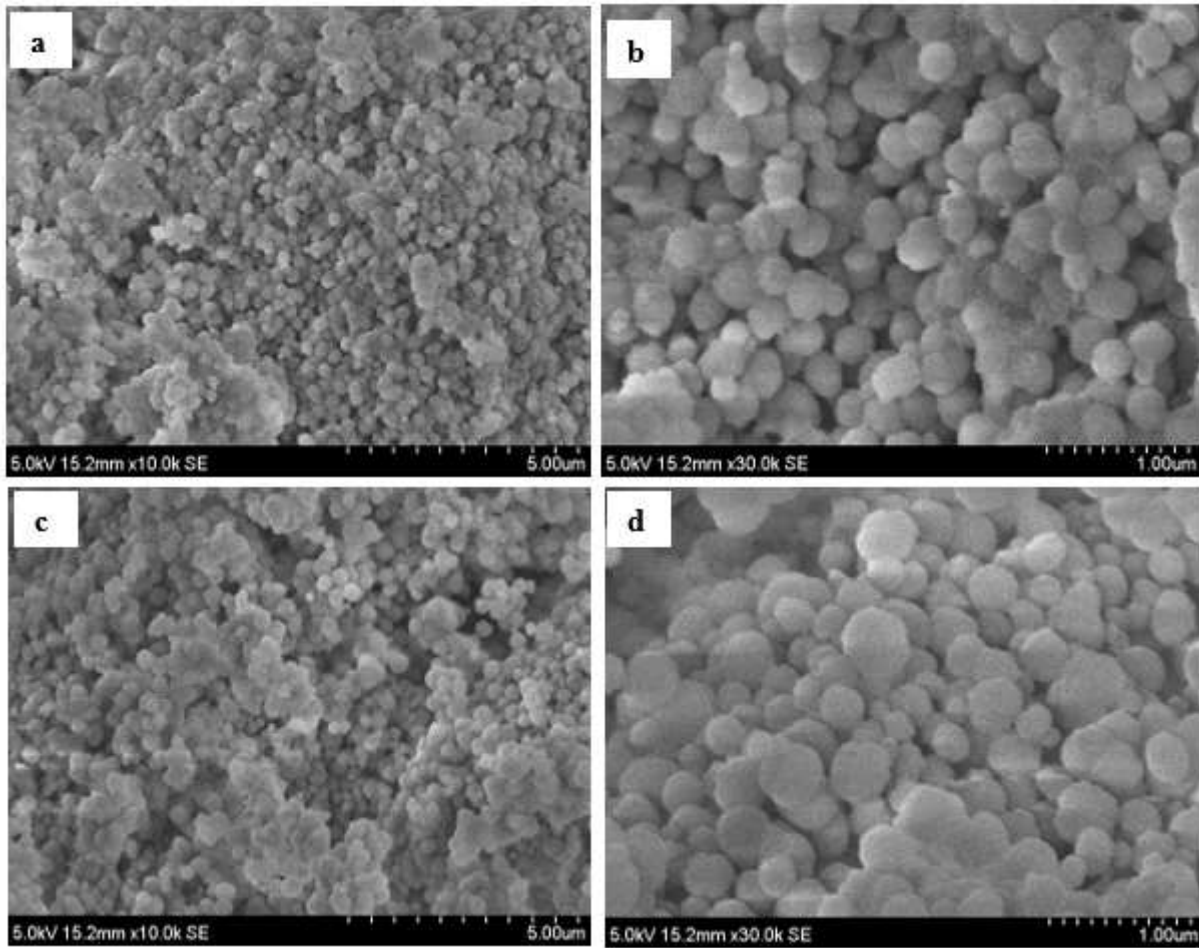


Figure 3

SEM micrographs of (a & b) conventional and (c & d) mesoporous silicalite-1

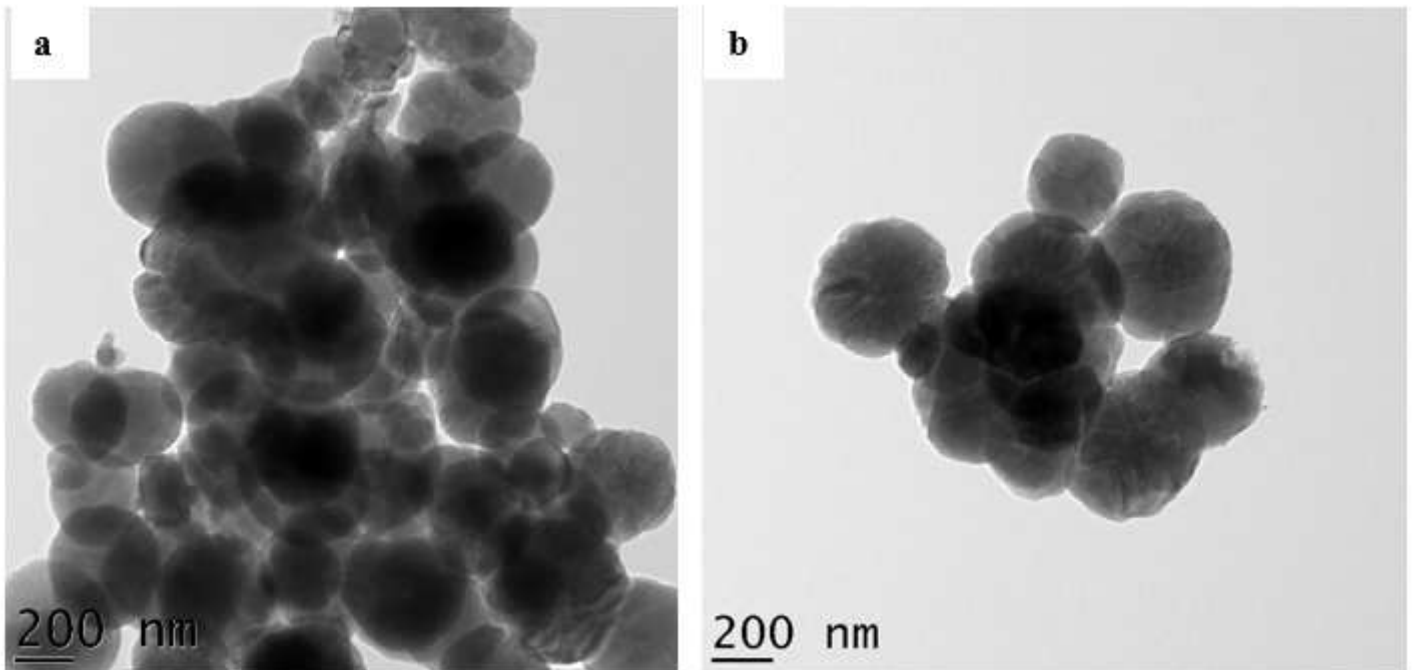


Figure 4

TEM images of mesoporous silicalite-1

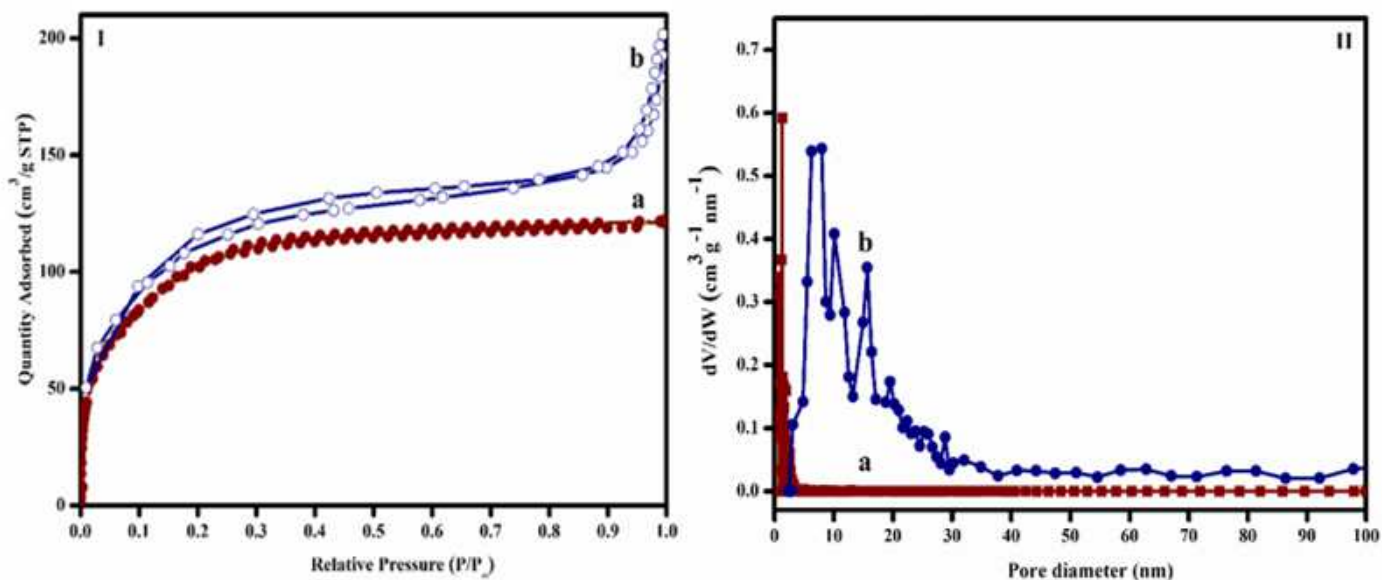


Figure 5

(I) N₂ adsorption isotherms of: a) conventional b) mesoporous silicalite-1; (II) pore size distribution of: a) conventional b) mesoporous silicalite-1

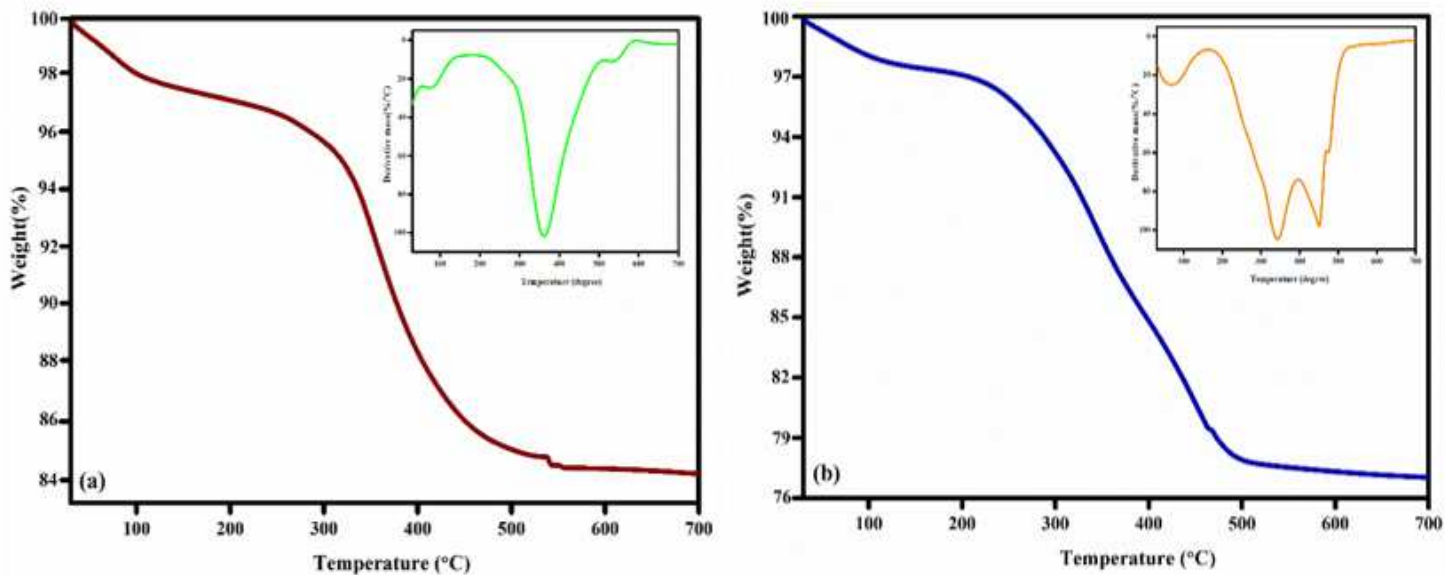


Figure 6

TGA curves of conventional and mesoporous silicalite-1 and the corresponding DTG curves are given at the inset

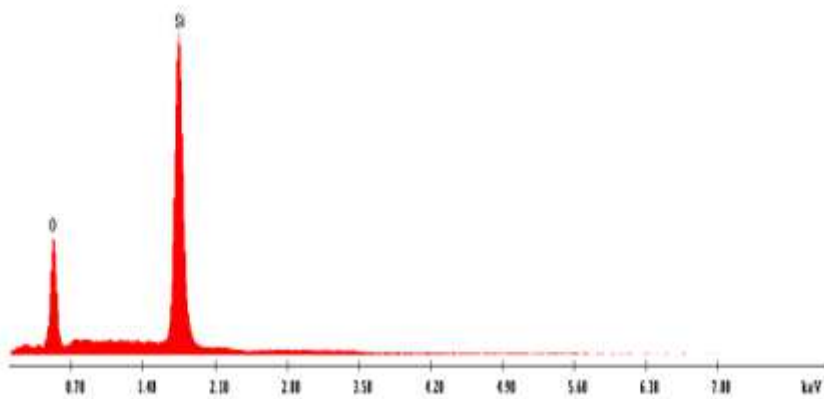


Figure 7

EDS image of mesoporous silicalite-1

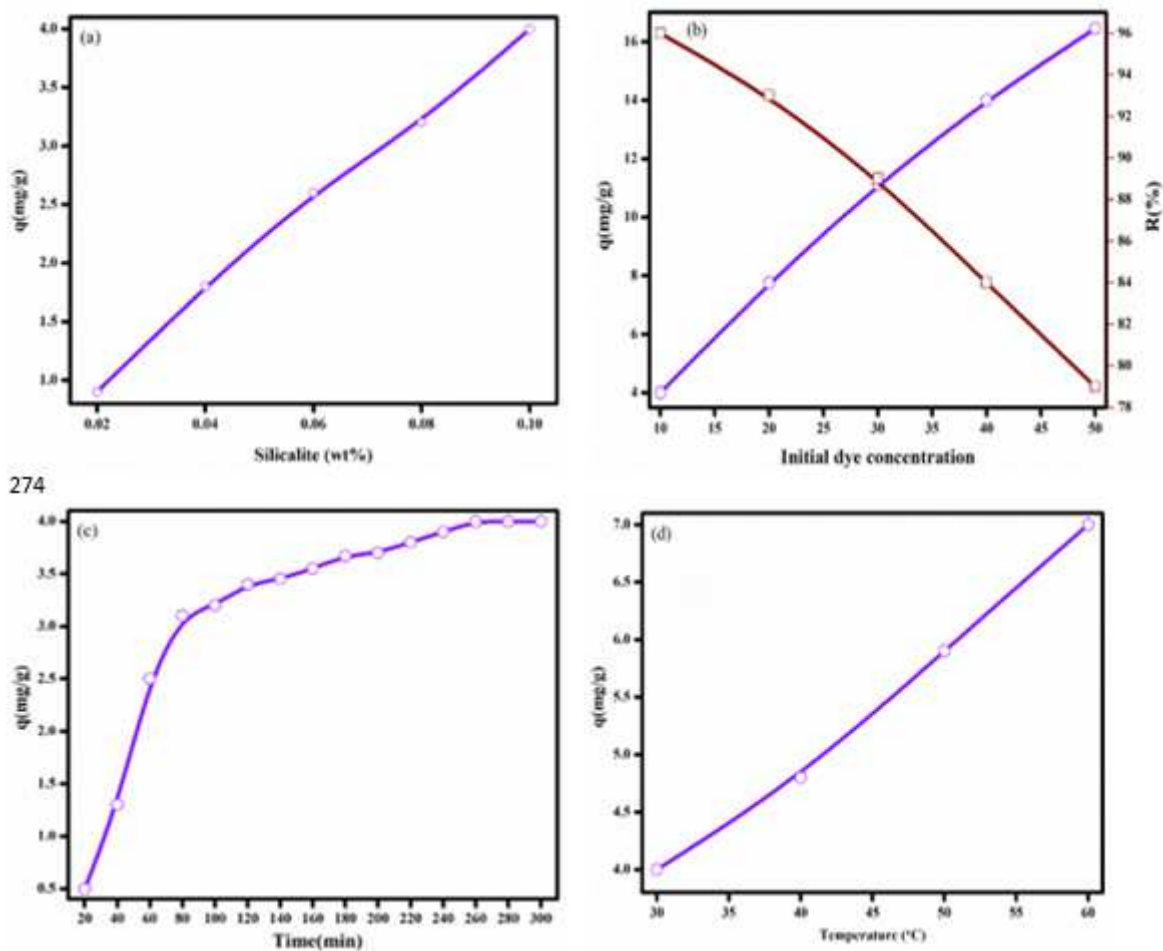


Figure 8

Effect of various parameters on the adsorption of MB onto mesoporous silicalite-1 a) silicalite-1 dosage b) initial dye concentration c) contact time d) temperature on the adsorption process (adsorbent dosage = 0.10 wt%, initial MO concentration = 10 ppm, contact time = 240 min and temperature = 30°C)

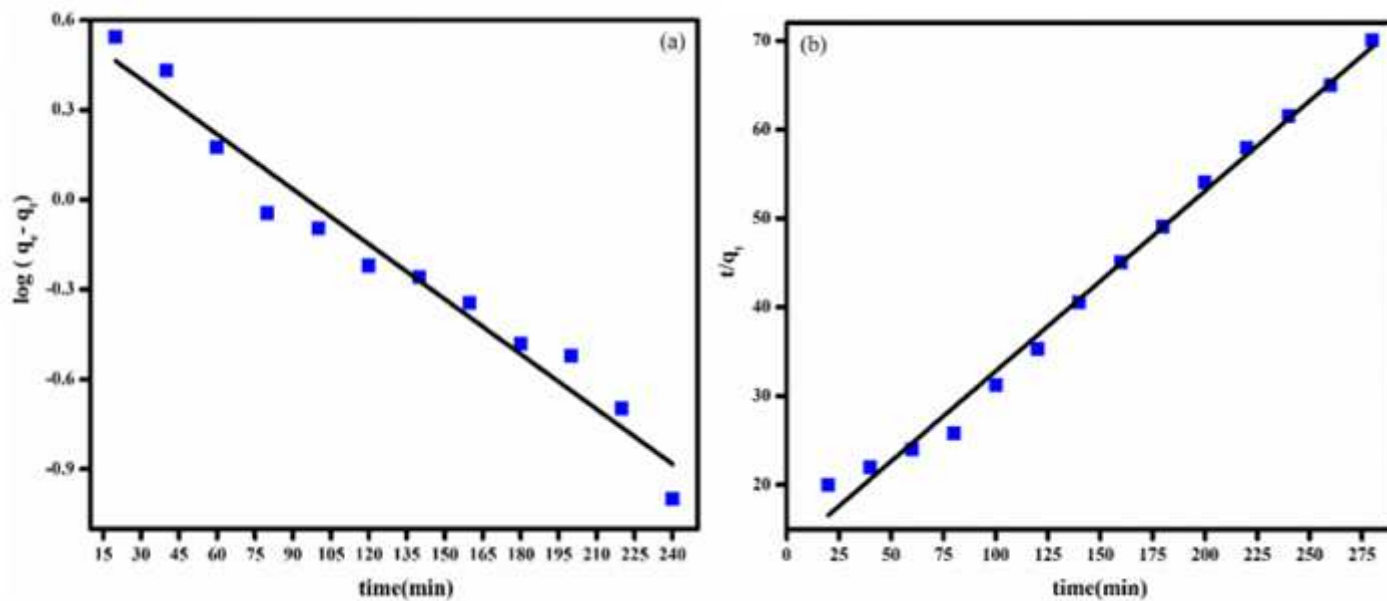


Figure 9

a) pseudo-first-order b) pseudo-second-order models for the adsorption of MB dye onto mesoporous silicalite-1

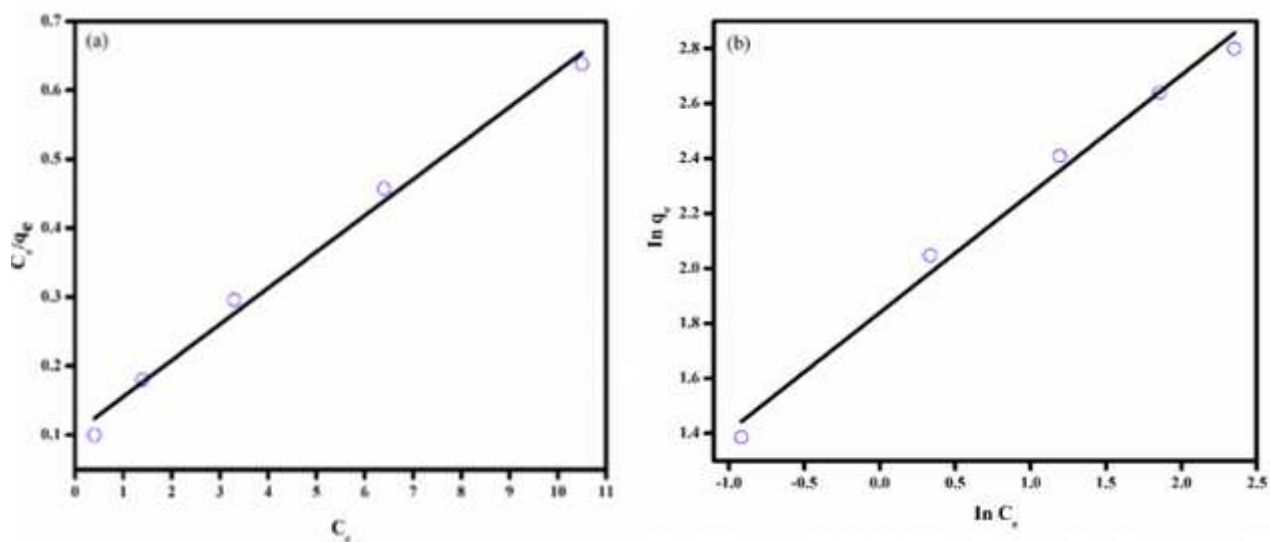


Figure 10

Isotherm model plots for the adsorption of MB a) Langmuir isotherm b) Freundlich isotherm

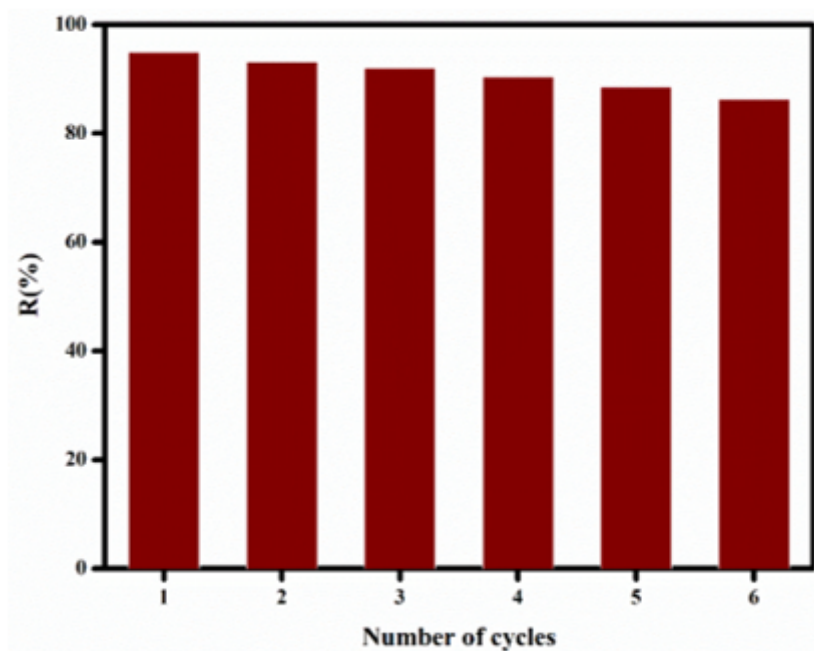


Figure 11

Reusability performance of adsorption of MB onto mesoporous silicalite-1

Supplementary Files

This is a list of supplementary files associated with this preprint. Click to download.

- [Graphicalabstract.docx](#)
- [Scheme1and2.docx](#)